DOI: 10.1002/ejic.200900424

Reactions of $[Et_4N][Tp^*W(\mu_3\text{-}S)(\mu\text{-}S)_2(CuSCN)_2]$ with Nitrogen Donor Ligands: Syntheses, Structures, and Third-Order Nonlinear Optical Properties

Zhen-Hong Wei,[a] Ling-Ling Li,[a] Zhi-Gang Ren,[a] Hong-Xi Li,[a] Jian-Ping Lang,*[a,b] Yong Zhang,[a] and Zhen-Rong Sun*[c]

Keywords: Tungsten / Copper / Cluster compounds / Sulfur / N ligands / Structure elucidation / Nonlinear optics

Reactions of the preformed cluster $[Et_4N][Tp^*W(\mu_3\text{-}S)(\mu\text{-}S)_2(CuSCN)_2]$ (**1**) with pyridine (py), 4,4′-bipyridine (4,4′-bipy), or 1,3-bis(4-pyridyl)propane (bpp) led to the formation of three neutral $[Tp^*W(\mu_3\text{-}S)(\mu\text{-}S)_2Cu_2]$-based compounds $[Tp^*W(\mu_3\text{-}S)(\mu\text{-}S)_2Cu_2(SCN)(py)_2]$ (**2**), $[\{Tp^*W(\mu_3\text{-}S)(\mu\text{-}S)_2Cu_2(SCN)\}_2(4,4'\text{-bipy})]\cdot 3.5H_2O$ (**3**·$3.5H_2O$), and $[Tp^*W(\mu_3\text{-}S)(\mu\text{-}S)_2Cu_2(SCN)(bpp)]_2$ (**4**), respectively. Compounds **2**–**4** were characterized by elemental analysis, IR spectra, UV/Vis spectra, ^1H NMR, and X-ray analysis. There are two linkage isomers $[Tp^*W(\mu_3\text{-}S)(\mu\text{-}S)_2Cu_2(SCN)(py)_2]$ and $[Tp^*W(\mu_3\text{-}S)(\mu\text{-}S)_2Cu_2(NCS)(py)_2]$, each of which has its own enantiomeric pair in the crystal of **2**. Compound **3** has a double butterfly-shaped structure in which two $[Tp^*W(\mu_3\text{-}S)(\mu\text{-}S)_2Cu_2(SCN)]$ fragments are linked with a single 4,4′-bipy bridge. For **4**, the two butterfly-shaped $[Tp^*W(\mu_3\text{-}S)(\mu\text{-}S)_2Cu_2(SCN)]$ fragments are interconnected by a pair of bpp bridges. The third-order nonlinear optical (NLO) performances of **2**–**4** in DMF were also investigated by *Z*-scan techniques.

Introduction

In the past decades, two metal–sulfur synthons $[ME_xS_{4-x}]^{2-}$ and $[Cp^*MS_3]^-$ (E = O, S; x = 0–3; Cp* = pentamethylcyclopentadienyl; M = Mo, W) were employed to react with copper(I) halide or pseudohalide such as CuBr, CuCN, and CuNCS due to their intriguing structures,[1] potential applications in biological systems[2] and optoelectronic materials.[1e,1g,1h,3] Among the known cluster modules, the incomplete cubane-like (Scheme 1, a) and the complete cubane-like clusters (Scheme 1, b) with terminal halides or pseudohalides coordinated at copper(I) atoms were found to be useful building blocks for the preparation of cluster-supported compounds.[1,4] For example, the incomplete cubane-like precursors $[Et_4N]_2[MOS_3Cu_3X_3]$ and $[PPh_4][Cp^*M(\mu_3\text{-}S)_3(CuX)_3]$ (M = Mo, W; X = CN, SCN, Br) were extensively employed to react with P- or N-donor ligands, and many discrete and supramolecular compounds with intriguing 1D, 2D, and 3D topological structures have been isolated.[5] It is noted that the third-order nonlinear optical (NLO) performances of some cluster precursors were improved when they were assembled into cluster-based species.[3] However, few papers have reported using the butterfly-shaped clusters (Scheme 1, c) to react with N-donor ligands to produce new cluster-based compounds with better NLO effects.[6]

Recently, we have been interested in the construction of Mo(W)/Cu/S clusters from the third synthon $[Et_4N][Tp^*WS_3]$ (Tp* = hydridotris(3,5-dimethylpyrazol-1-yl)borate),[7] and a new family of W/Cu/S clusters with various frameworks were obtained.[8] The incomplete cubane-like core cluster $[Et_4N][Tp^*W(\mu_3\text{-}S)_3(CuBr)_3]$ was treated with mono- and bidentate nitrogen donor ligands.[9] To expand the chemistry of the W/Cu/S cluster bearing the $[Tp^*WS_3]$ moiety and screen out those with better third-order NLO properties, a precursor cluster with a butterfly-shaped structure $[Et_4N][Tp^*W(\mu_3\text{-}S)(\mu\text{-}S)_2(CuSCN)_2]$ (**1**)[9b] was employed to react with three N-donor ligands that include a monodentate ligand pyridine (py), a rigid bidentate ligand 4,4′-bipyridine (4,4′-bipy), and a flexible bidentate ligand 1,3-bis(4-pyridyl)propane (bpp). Three neutral clusters $[Tp^*W(\mu_3\text{-}S)(\mu\text{-}S)_2Cu_2(SCN)(py)_2]$ (**2**), $[\{Tp^*W(\mu_3\text{-}S)(\mu\text{-}S)_2Cu_2(SCN)\}_2(4,4'\text{-bipy})]\cdot 3.5H_2O$ (**3**·$3.5H_2O$), and $[Tp^*W(\mu_3\text{-}S)(\mu\text{-}S)_2Cu_2(SCN)(bpp)]_2$ (**4**) were isolated. Compounds **2**–**4** were also confirmed to exhibit good third-order NLO performances in DMF through *Z*-scan techniques with an 80-fs pulse width at 800 nm. Herein, we report their syntheses, crystal structures, and third-order NLO properties.

[a] Key Laboratory of Organic Synthesis of Jiangsu Province, College of Chemisty, Chemical Engineering and Materials Science, Suzhou University,
Suzhou 215123, Jiangsu, P. R. China
Fax: +86-512-65880089
E-mail: jplang@suda.edu.cn
[b] State Key Laboratory of Organometallic Chemistry, Shanghai Institute of Organic Chemisty, Chinese Academy of Sciences, Shanghai 200032, P. R. China
[c] State Key Laboratory of Precision Spectroscopy and Department of Physics, East China Normal Univerity, Shanghai 200062, P. R. China

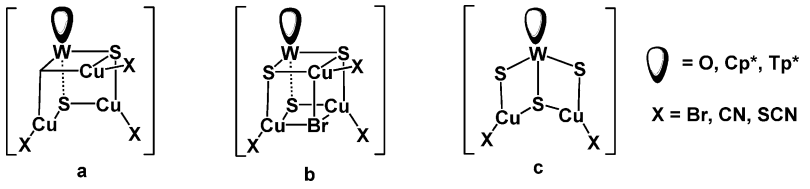

Scheme 1. The precursor clusters with an incomplete cubane-like core (a), a complete cubane-like core (b), or a butterfly-shaped core (c) structure.

Results and Discussion

Synthesis and Characterization

As shown in Scheme 2, the reactions of **1** with N-donor ligands were straightforward. Treatment of **1** with excess py afforded **2** in 72% yield. Because of the existence of two different coordination modes of the thiocyanate ligand, crystals of **2** were a mixture with a 1:1 molar ratio of two linkage isomers $[Tp^*W(\mu_3\text{-}S)(\mu\text{-}S)_2Cu_2(SCN)(py)_2]$ and $[Tp^*W(\mu_3\text{-}S)(\mu\text{-}S)_2Cu_2(NCS)(py)_2]$. We assumed that two py ligands may first replace two NCS groups to form a $[Tp^*W(\mu_3\text{-}S)(\mu\text{-}S)_2Cu_2]^+$ cation. This cation may be further coordinated by the thiocyanate group via either its N-end or its S-end, which may understandably form two linkage isomers in an equal ratio. It is noted that the reaction involved in the change of the coordination modes of the thiocyanate group is rare.[5e] Reactions of **1** in MeCN with three equiv. of 4,4′-bipy gave rise to a dimeric neutral cluster **3**·3.5H_2O in 45% yield while analogous reactions of **1** with bpp produced the other dimeric cluster **4** in 50% yield. Compounds **2**–**4** are relatively air and moisture stable in the solid state, and are soluble in MeCN, DMSO, and DMF. The IR spectra of **2**–**4** displayed a band of the bridging W–S stretching vibration at 421 (**2**), 439 (**3**), or 423 (**4**) cm^{-1}, a band of the B–H stretching vibration at ca. 2564 cm^{-1}, and a band of the thiocyanate stretching vibration at ca. 2094 cm^{-1}. The ^1H NMR spectra of **2**–**4** in $CDCl_3$ or $[D_6]$-DMSO at room temperature displayed two sharp singlets with the same intensities at ca. 2.37/2.95 ppm, and one singlet at ca. 6.00 ppm, which were assigned to the methyl protons and the pyrazolyl methine protons of the Tp* groups, respectively. In addition, two double peaks at 8.56–8.53, 7.79–7.75 ppm, and a triple peak at 7.41–7.35 ppm for pyridyl protons of pyridine (**2**); two double peaks at 8.54–8.46, 7.59–7.54 ppm for pyridyl protons of 4,4′-bipy (**3**); two double peaks at 8.50–8.49, and 7.35–7.34 ppm for pyridyl protons, and a double peak at 2.50–2.48 ppm and multiple peaks at ca. 1.96 ppm for the methylene protons of bpp (**4**) were also observed. The UV/Vis spectrum of **1** in MeCN was characterized by two bands, while those of **2**–**4** had three absorptions (Figure 1). Relative to the bands at 297 and 403 nm for **1**, those at 315, 433, and 472 nm for **2**–**4** are red-shifted, and they are probably dominated by the $S\rightarrow W^{VI}$ charge-transfer transitions of the $[Tp^*WS_3]$ moiety.[9] The identities of **2**–**4** were further confirmed by X-ray crystallography.

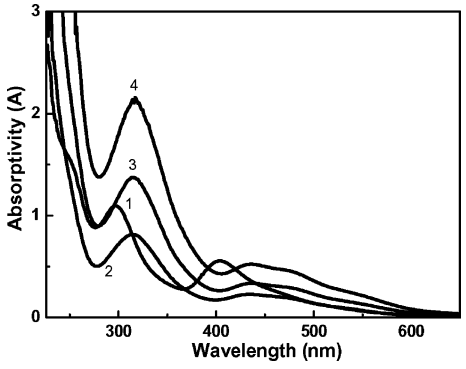

Figure 1. Electronic spectra of **1** (4.5×10^{-5} M), **2** (2.8×10^{-5} M), **3** (3.6×10^{-5} M), and **4** (4.0×10^{-5} M) in DMF in a 1-cm thick glass cell.

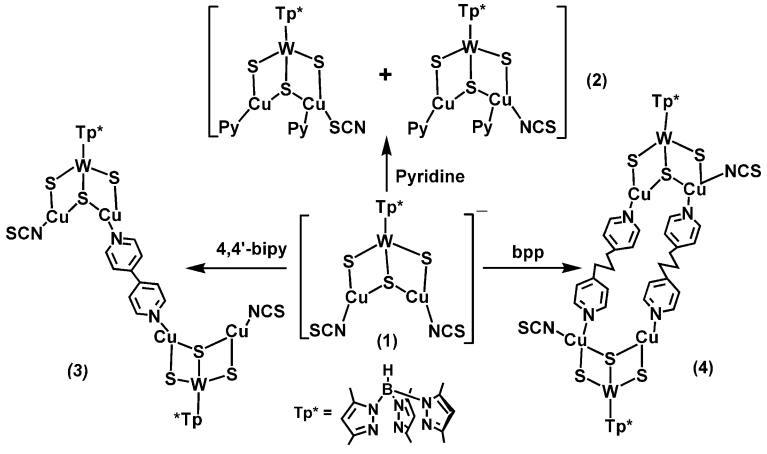

Scheme 2. Reactions of **1** with py, 4,4′-bipy, and bpp ligands.

Crystal Structure of $[Tp^*W(\mu_3\text{-}S)(\mu\text{-}S)_2Cu_2(SCN)(py)_2]$ (2)

Compound **2** crystallized in the monoclinic space group $P2_1/n$, and the asymmetric unit contains two discrete molecules $[Tp^*WS_3Cu_2(NCS)(py)_2]$ and $[Tp^*WS_3Cu_2(SCN)(py)_2]$. As shown in Figure 2, the two structures are almost the same except for the different coordinated modes of the thiocyanate ligand to the Cu atom. In one cluster *a*, the thiocyanate ligand binds to Cu(2) via its S atom, while in the other *b*, the thiocyanate coordinates at Cu(4) via its N atom. There are numerous examples showing that the terminal thiocyanate tends to bind at the Cu^I center via its N-end. However, a limited number of copper(I)/thiocyanate complexes were reported to have their terminal thiocyanate coordinate at copper(I) centers via its S-end.[5e] While in compound **2**, the NCS^- ions are coordinated to Cu atoms through both N and S atoms exhibiting linkage isomerism. This is the only example of linkage isomers structurally characterized in W/Cu thiocyanato complexes.

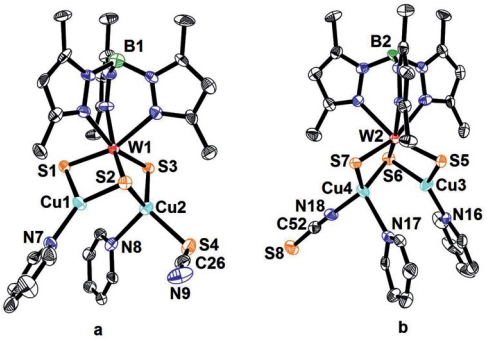

Figure 2. (a) View of the molecular structure of the cluster *a* in **2**. (b) View of the molecular structure of the cluster *b* in **2**. Thermal ellipsoids are drawn at 30% probability level and all hydrogen atoms are omitted for clarity.

Each unit keeps the butterfly-shaped $[Tp^*WS_3Cu_2]$ core structure of **1**. The oxidation states of the W and Cu centers (+6 and +1, respectively) in **1** were also retained in **2**. However, the two Cu^I atoms in each unit adopt different coordination geometries. Cu(1) or Cu(3) adopts a trigonal planar environment, coordinated by one μ-S, one μ_3-S, and one N from the py ligand. Cu(2) or Cu(4) are tetrahedrally coordinated by one μ-S, one μ_3-S, one N atom of the bpp ligand and one S atom of the SCN ligand [Cu(2)] or one N atom of the NCS ligand [Cu(4)]. For the trigonally coordinated Cu(1) or Cu(3), their mean W···Cu contact [2.6016(19) Å] (Table 1) is shorter than those of **1** [2.6404(11) Å] and $[PPh_4][Cp^*WS_3(CuCN)_2]$ [2.666(3) Å].[10a] For the tetrahedrally coordinated Cu(2) or Cu(4), their mean W···Cu contact [2.6720(18) Å] is almost the same as that of $[WS_4Cu_2(py)_4]$ [2.6711(6) Å],[10b] but shorter than that of $[PPh_4][\{Cp^*WS_3Cu_2(py)(CN)\}_2(\mu\text{-}CN)]$ [2.714(2) Å].[10a] The mean Cu–N(py) length at 1.920(12) Å is shorter than that of Cu–N(NCS) [2.311(12) Å]. The W-μ-S, W-μ_3-S, Cu-μ_3-S, and Cu-μ-S bond lengths are normal.

It is noted that the asymmetric environment of Cu(2) or Cu(4) leads to the introduction of asymmetry in the metal–sulfur core, which results in the formation of the two different chiral clusters *a* and *b*. However, in the packing of **2** (Figure 3), both cluster *a* and cluster *b* are found in their enantiomeric forms. That means that one crystal contains two different racemic mixtures of two pairs of cluster enantiomers and crystal **2** is achiral with a monoclinic space group $P2_1/n$.

Table 1. Selected bond lengths [Å] for **2**–**4**.

Compound **2**			
Cluster a			
W(1)···Cu(1)	2.6075(19)	W(1)···Cu(2)	2.6767(18)
W(1)–S(1)	2.238(3)	W(1)–S(3)	2.238(3)
W(1)–S(2)	2.306(4)	Cu(1)–S(1)	2.182(4)
Cu(1)–S(2)	2.216(4)	Cu(2)–S(3)	2.241(4)
Cu(2)–S(2)	2.254(4)	Cu(2)–S(4)	2.260(4)
Cu(1)–N(7)	1.950(12)	Cu(2)–N(8)	2.311(12)
Cluster b			
W(2)···Cu(3)	2.5957(19)	W(2)···Cu(4)	2.6674(18)
W(2)–S(5)	2.238(3)	W(2)–S(6)	2.213(4)
W(2)–S(7)	2.223(3)	Cu(3)–S(6)	2.182(4)
Cu(3)–S(5)	2.177(4)	Cu(4)–S(6)	2.263(4)
Cu(4)–S(7)	2.231(4)	Cu(2)–S(4)	2.260(4)
Cu(3)–N(16)	1.916(8)	Cu(4)–N(18)	1.895(12)
Compound **3**			
W(1)···Cu(1)	2.6507(14)	W(1)···Cu(2)	2.6305(13)
W(1)–S(1)	2.231(2)	W(1)–S(2)	2.318(2)
W(1)–S(3)	2.241(2)	Cu(1)–S(1)	2.219(3)
Cu(1)–S(2)	2.251(3)	Cu(2)–S(3)	2.204(3)
Cu(2)–S(2)	2.214(3)	Cu(1)–N(8)	1.903(9)
Cu(2)–N(7)	1.950(7)		
Compound **4**			
W(1)···Cu(1)	2.6718(15)	W(1)···Cu(2)	2.6038(16)
W(1)–S(1)	2.222(3)	W(1)–S(2)	2.327(3)
W(1)–S(3)	2.249(3)	Cu(1)–S(1)	2.244(3)
Cu(1)–S(2)	2.266(3)	Cu(2)–S(3)	2.173(3)
Cu(2)–S(2)	2.202(3)	Cu(1)–N(7)	1.928(9)
Cu(1)–N(8)	2.279(10)	Cu(2)–N(9)	1.930(15)

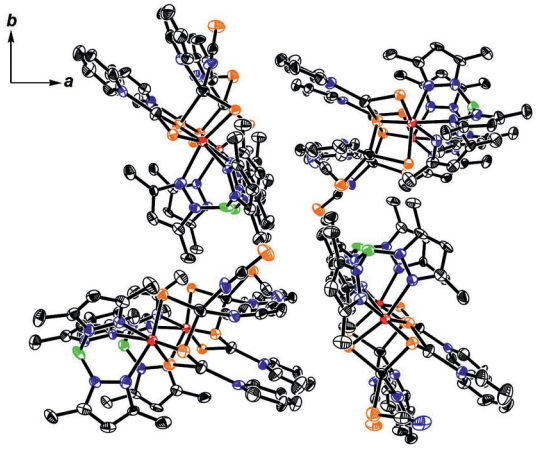

Figure 3. The packing view of **2** looking along the *c*-axis. All hydrogen atoms are omitted for clarity.

As the separations of the S-end and N-end in each thiocyanate to the Cu^I atoms in the adjacent clusters in **2** are Cu4···S8 4.653(4) Å, Cu2···N9 3.991(4) Å, each thiocyanate

only works as a monodentate ligand, and is not involved in secondary interactions with trigonally coordinated Cu^I atoms to form polymeric species.

Crystal Structures of [{Tp*W(μ$_3$-S)(μ-S)$_2$Cu$_2$(NCS)}$_2$-(4,4′-bipy)]·3.5H$_2$O (3·3.5H$_2$O) and [Tp*W(μ$_3$-S)(μ-S)$_2$Cu$_2$-(NCS)(bpp)]$_2$ (4)

Compound **3**·3.5H_2O crystallized in the triclinic space group $P\bar{1}$, and the asymmetric unit contains half of the [{Tp*WS_3Cu_2(NCS)}$_2$(4,4′-bipy)] molecule and three halves and one quarter of water-solvent molecules. Compound **4** crystallizes in the triclinic space group $P\bar{1}$, and the asymmetric unit contains half of the neutral molecule [Tp*WS_3Cu_2(NCS)(bpp)]$_2$. Compound **3** is composed of two butterfly-shaped [Tp*W(μ-S)$_2$(μ$_3$-S)Cu_2(NCS)] fragments linked by a bridging 4,4′-bipy ligand, forming a type of double butterfly-shaped structure. There is a crystallographic center of symmetry located on the middle point of the C(20)–C(20A) bond (Figure 4, a). Compound **4** has a different type of double butterfly-shaped structure in which two [Tp*W(μ-S)$_2$(μ$_3$-S)Cu_2(NCS)] fragments are connected by a pair of bpp bridges. There is also a crystallographic center of symmetry located on the middle point of the W(1) and W(1A) contact (Figure 4, b). The different types of double butterfly-shaped structures of **3** and **4** may be due to the different flexibility that bpp and 4,4′-bipy possess. The bpp ligand is more flexible than the 4,4′-bipy ligand, and it may more easily adjust its conformation to coordinate more Cu^I centers to form a more complicated double butterfly-shaped structure.

In each [Tp*W(μ-S)$_2$(μ$_3$-S)Cu_2(NCS)] fragment of **3**, each copper atom adopts a trigonal planar geometry, coordinated by one μ-S, one μ$_3$-S, and one N from the NCS ligand [Cu(1)], or one N from the 4,4′-bipy ligand [Cu(2)]. The W(1)···Cu(1) contact is slightly longer than that of W(1)···Cu(2). Their mean value [2.6406(13) Å] is almost the same as that of **1**, but longer than that of **2**. The Cu–N(4,4′-bipy) length at 1.950(7) Å is longer than that of **2**. The W-μ-S, W-μ$_3$-S, Cu-μ$_3$-S, and Cu-μ-S bond lengths are normal relative to the corresponding ones in **1**. In addition, the S atom of the thiocyanate in each [Tp*W(μ-S)$_2$(μ$_3$-S)-Cu_2(NCS)] fragment has the weak interactions with the two Cu atoms in the next fragment [Cu(1A)–S(4) = 2.813(5) Å and Cu(2A)–S(4) = 2.928(5) Å], thereby forming a 1D zigzag chain (Figure 5).

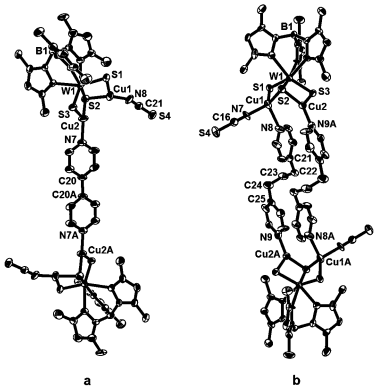

Figure 4. (a) View of the molecular structure of **3** with 30% thermal ellipsoid. Symmetry code: A, –*x* + 3, –*y*, –*z* + 1. (b) View of the molecular structure of **4** with 30% thermal ellipsoid. Symmetry code: A, –*x*, –*y*, –*z* + 2. All hydrogen atoms are omitted for clarity.

On the other hand, in each [Tp*W(μ-S)$_2$(μ$_3$-S)Cu_2(NCS)] fragment of **4**, Cu(2) adopts a trigonal planar geometry, coordinated by one μ-S, one μ$_3$-S, and one N from the bpp ligand, while the other is tetrahedrally coordinated by one μ-S, one μ$_3$-S, one N from NCS, and one N of the bpp ligand [Cu(2)]. Because of the asymmetric environment of Cu(2), each fragment behaves chirally. However, the two fragments are related by an inversion center located at the center of the structure. Thus, cluster **4** itself is a meso-isomer. For the trigonally coordinated Cu and the tetrahedrally coordinated Cu, the W···Cu contacts [2.6038(16) Å vs. 2.6718(15) Å] in **4** are comparable to those of the corresponding ones of **2**. The W-μ-S, W-μ$_3$-S, Cu-μ$_3$-S, Cu-μ-S,

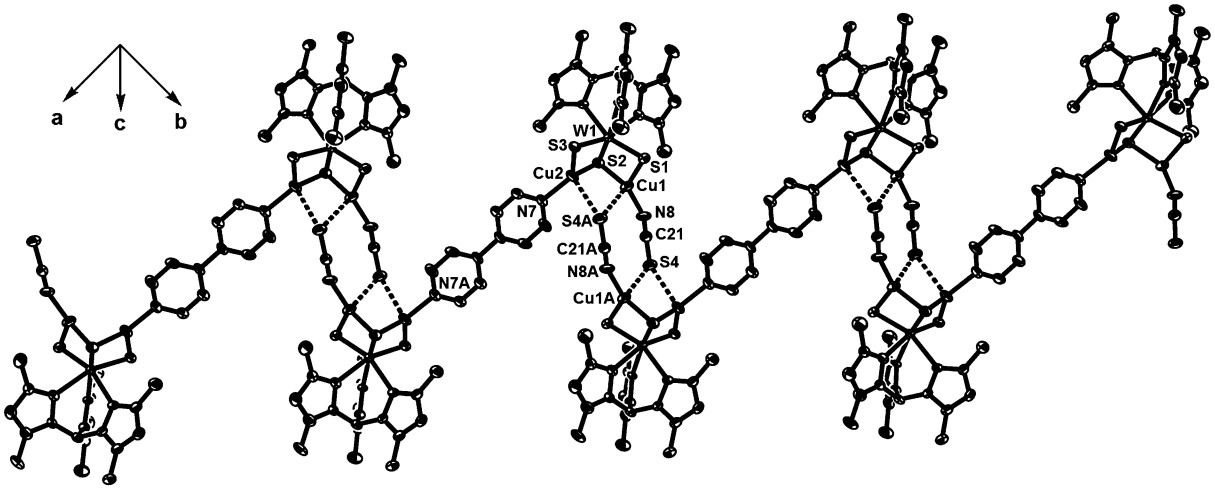

Figure 5. View of a section of the 1D zigzag chain of **3** formed by weak Cu···SCN interactions.

Cu–N(bpp), and Cu–N(NCS) bond lengths are normal. Each bpp ligand in **4** has a *trans-gauche* conformation. Interestingly, this dimeric cluster is ca. 2.7 nm long in one direction (from C1 to C1A), and thus may be viewed as a nanoscale cluster, which is almost as long as the reported cluster [{Tp*W(μ_3-S)$_3$Cu$_3$Br$_2$}$_2$(bpee)] (2.9 nm).[9a]

Third-Order Nonlinear Optical Properties of 2–4

As indicated in Figure 1, the electronic spectra of **2**–**4** in DMF showed relatively low linear absorption at 800 nm, which promises low intensity loss and little temperature change by photon absorption during the NLO measurements. The nonlinear absorption performances of **2**–**4** in DMF were evaluated by the Z-scan technique under an open aperture configuration (Figure 6, a). Although the detailed mechanism is still unknown, the NLO absorption data obtained under the conditions used in this study can be evaluated from the reported methods.[11] The data collected under the open-aperture configuration indicate that they all exhibit good nonlinear absorption properties with effective α_2 values of 6.2×10^{-12} m W^{-1} (**2**), 6.1×10^{-12} m W^{-1} (**3**), and 5.5×10^{-12} m W^{-1} (**4**). The nonlinear refractive properties of **2**–**4** were assessed by dividing the normalized *Z*-scan data obtained under closed aperture by the normalized *Z*-scan data collected under the open aperture configuration (Figure 6, b). According to literature methods,[12,13] the effective third-order NLO refractive index n_2 values are 5.7×10^{-12} esu (**2**), 7.0×10^{-12} esu (**3**), and 6.5×10^{-12} esu (**4**), respectively.[14] In accordance with the observed α_2 and n_2 values, the effective third-order susceptibilities $\chi^{(3)}$ for **2**–**4** are calculated to be 3.1×10^{-14} esu (**2**), 3.8×10^{-14} esu (**3**), and 4.0×10^{-14} esu (**4**) while the corresponding second-order hyperpolarizability γ values are 3.6×10^{-32} esu (**2**), 6.3×10^{-32} esu (**3**), and 4.8×10^{-32} esu (**4**), respectively. These results showed that **2**–**4** possess relatively strong third-order optical nonlinearities.

The γ value can be used to represent NLO properties of neat materials. When compared with nanosecond and picosecond measurement values, femtosecond values are roughly 2–3 orders of magnitude lower.[15] The γ values of **2**–**4** are comparable to those of other M/Cu/S clusters derived from $[MS_4]^{2-}$, $[MOS_3]^{2-}$, $[Cp^*MS_3]^-$, and $[Tp^*MS_3]^-$ (M = Mo, W), such as $[(Et_4N)_2\{WS_4Cu_4(CN)_4\}]_n$ (1.26×10^{-29} esu),[3e] $[MoS_4Cu_4(\alpha\text{-MePy})_5Br_2]\cdot2(\alpha\text{-MePy})_{0.5}$ (1.06×10^{-30} esu),[16a] $[(n\text{Bu})_4N]_2[MoOS_3(CuNCS)_3]$ (4.8×10^{-29} esu),[16b] $[WOS_3Cu_3(4\text{-MePy})_6](BF_4)$ (4.43×10^{-31} esu),[16c] $[WOS_3Cu_2(4\text{-}t\text{BuPy})_2]_2$ (4.8×10^{-30} esu),[16d] $\{[(Cp^*MoS_3Cu_3)_2(\mu\text{-bpp})_3(\mu\text{-NCS})_2(NCS)](NCS)\}_n$ [bpp = 1,3-bis(4-pyridyl)propane, 3.86×10^{-29} esu],[5g] $[Et_4N]_2$-$[Tp^*W(\mu_3\text{-S})_3(CuNCS)_3(\mu_3\text{-Br})]\cdot1.5$aniline ($3.6\times10^{-32}$ esu), and $\{[Et_4N][Tp^*W(\mu_3\text{-S})_3(Cu\text{-}\mu\text{-SCN})_3(Cu\text{-}\mu_3\text{-NCS})]\}_n$ (4.6×10^{-32} esu).[9b] It is noted that the γ values of **2**–**4** are 1.2–2.2-times larger than that of **1** (2.9×10^{-32} esu).[9b] Such an enhancement may be attributed to the peripheral ligands around the cluster cores and possibly the skeletal expansion of the cluster.[4i] The γ values of the dimeric clusters **3**–**4** were larger than those of the single clusters **1** and **2** due to the existence of two single cubane-like cluster cores in **3**–**4**.

Conclusions

In this paper, we have demonstrated the reactivity of the precursor cluster **1** towards py, 4,4′-bipy, and bpp, and successful isolation of three neutral clusters **2**–**4**. According to X-ray analysis, **2** consists of two linkage isomers [Tp*W(μ_3-S)(μ-S)$_2$Cu$_2$(μ-SCN)(py)$_2$] and [Tp*W(μ_3-S)(μ-S)$_2$Cu$_2$(μ-NCS)(py)$_2$], each of which has its own enantiomer in the

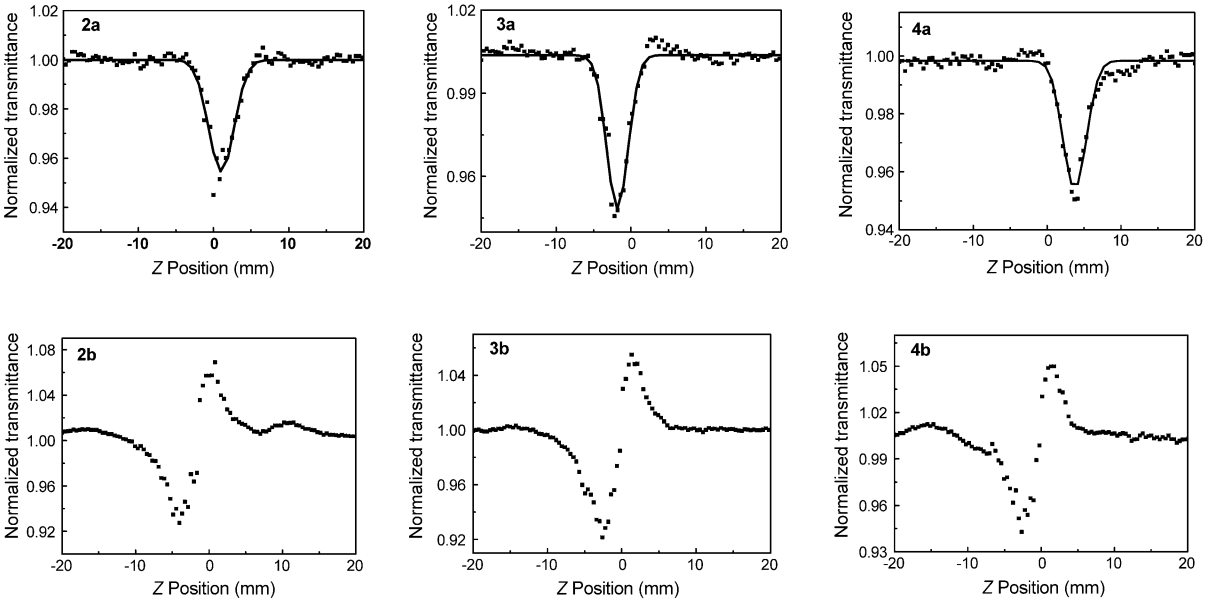

Figure 6. *Z*-scan data of DMF solutions of **2**–**4** with 80-fs laser pulses and 1.5-mm cell. (a) The data were evaluated under open-aperture configuration. (b) The data were assessed by dividing the normalized Z-scan data obtained under the closed aperture by the normalized *Z*-scan data in (a). The black dots are experimental data, and the black solid curve is the theoretical fit.

crystal. The formation of the two isomers may be involved in the unusual conversion of the coordination modes of the thiocyanate group from its N-end to its S-end. Compounds **3** and **4** have two kinds of double butterfly-shaped structures, in which two [Tp*W(μ_3-S)(μ-S)$_2$Cu$_2$(SCN)] fragments are interconnected either via a single 4,4′-bipy bridge (in **3**) or a pair of bpp bridges (in **4**). Compounds **2**–**4** show better third-order NLO performances than their precursor **1**. These results revealed that **1** is an excellent structural and NLO precursor for W/Cu/S cluster-based assemblies. Further work on the rational design and assembly of new [Tp*WS$_3$Cu$_2$]-based arrays from reactions of **1** with other multidentate N-donor ligands and the improvement of their NLO performances is under way in this laboratory.

Experimental Section

General Remarks: All manipulations were performed under an argon atmosphere using standard Schlenk-line techniques. Compound **1** was prepared as reported previously.[9b] All solvents were predried with activated molecular sieves and refluxed over the appropriate drying agents under argon. ^{1}H NMR spectra were recorded at ambient temperature with a Varian UNITYplus-400 spectrometer. ^{1}H NMR chemical shifts were referenced to TMS in $CDCl_3$ signal. IR spectra were recorded with a Varian 1000 FT-IR spectrometer as KBr disks (4000–400 cm^{-1}). UV/Vis spectra were measured with a Varian 50 UV/Vis spectrophotometer. Elemental analyses for C, H, and N were performed with a Carlo–Erba CHNO-S microanalyzer.

[Tp*W(μ_3-S)(μ-S)$_2$Cu$_2$(SCN)(py)$_2$] (2): To a pyridine solution (5 mL) was added **1** (53 mg, 0.05 mmol). After being stirred for half an hour, the resulting red solution was filtered and Et_2O (10.0 mL) was carefully layered onto the surface of the filtrate. Dark red blocks of **2** were formed two days later, which were collected by filtration, washed with Et_2O, and dried in vacuo; yield 33 mg (72% based on **1**). $C_{26}H_{32}BCu_2N_9S_4W$ (920.64): calcd. C 33.92, H 3.51, N 13.70; found C 34.36, H 3.41, N 13.36. IR (KBr disk): $\tilde{\nu}$ = 2965 (w), 2921 (s), 2561 (w), 2100 (s), 1605 (w), 1544 (s), 1448 (m), 1413 (s), 1354 (m), 1216 (s), 1070 (s), 1033 (s), 860 (m), 820 (m), 751 (m), 694 (m), 650 (w), 477 (w), 421 (w) cm^{-1}. UV/Vis (MeCN): λ_{max} (ε, M^{-1}cm^{-1}) = 315 (15900), 434 (4500), 471 (3500) nm. ^{1}H NMR (400 MHz, $CDCl_3$): δ = 2.37 (s, 9 H, CH_3 in Tp*), 2.80 (s, 9 H, CH_3 in Tp*), 6.09 (s, 3 H, CH in Tp*), 7.41–7.35 (t, 4 H, CH in Py), 7.79–7.75 (t, 2 H, CH in Py), 8.56–8.53 (t, 4 H, CH in Py) ppm; the B-H proton signal was not located.

[{Tp*W(μ_3-S)(μ-S)$_2$Cu$_2$(NCS)}$_2$(4,4′-bipy)]·3.5H$_2$O (3·3.5H$_2$O): To a solution of **1** (53 mg, 0.05 mmol) in MeCN (5 mL) was added 4,4′-bipy (23 mg, 0.15 mmol). A workup similar to that used for the isolation of **2** afforded deep red blocks of **3** two weeks later, which were collected by filtration, washed thoroughly with Et_2O, and dried in vacuo; yield 39 mg (45% based on **1**). $C_{42}H_{59}B_2Cu_4N_{16}O_{3.5}S_8W_2$ (1744.16): calcd. C 28.92, H 3.42, N 12.85; found C 29.22, H 3.23, N 12.36. IR (KBr disk): $\tilde{\nu}$ = 2976 (w), 2928 (w), 2564 (w), 2094 (m), 1615 (m), 1542 (m), 1481 (m), 1377 (s), 1220 (w), 1069 (s), 1034 (s), 809 (w), 689 (w), 528 (m), 439 (m) cm^{-1}. UV/Vis (MeCN: λ_{max} (ε, M^{-1}cm^{-1}) = 315 (25600), 436 (7000), 472 (6200) nm. ^{1}H NMR (400 MHz, $CDCl_3$): δ = 2.37 (s, 18 H, CH_3 in Tp*), 2.79 (s, 18 H, CH_3 in Tp*), 6.10 (s, 6 H, CH in Tp*), 7.59–7.54 (d, 4 H, CH in 4,4′-bipy), 8.54–8.46 (d, 4 H, CH in 4,4′-bipy) ppm; the B–H proton signal was not located.

[Tp*W(μ_3-S)(μ-S)$_2$Cu$_2$(NCS)(bpp)]$_2$ (4): To a solution of **1** (53 mg, 0.05 mmol) in MeCN (5 mL) was added bpp (30 mg, 0.15 mmol). A workup similar to that used for the isolation of **2** afforded deep red blocks of **4** two weeks later, which were collected by filtration, washed thoroughly with MeCN/Et_2O (v/v = 1:4), and dried in vacuo; yield 24 mg (50% based on **1**). $C_{58}H_{72}B_2Cu_4N_{18}S_8W_2$ (1921.40): calcd. C 36.25, H 3.79, N 13.13; found C 35.78, H 3.45, N 13.32. IR (KBr disk): $\tilde{\nu}$ = 2975 (w), 2924 (w), 2565 (w), 2105 (m), 1615 (m), 1542 (m), 1481 (m), 1377 (s), 1220 (w), 1069 (s), 1034 (s), 809 (w), 689 (w), 517 (w), 423 (w) cm^{-1}. UV/Vis (MeCN: λ_{max} (ε, M^{-1}cm^{-1}) = 317 (28600), 436 (6700), 478 (6100) nm. ^{1}H NMR (400 MHz, $CDCl_3$): δ = 1.96 (m 2 H,-CH_2- in bpp), 2.38 (s,

Table 2. Crystallographic data and structure refinement for **2**, **3**·3.5H$_2$O, and **4**.

	2	**3**·3.5H$_2$O	**4**
Chemical formula	$C_{26}H_{32}BCu_2N_9S_4W$	$C_{42}H_{59}B_2Cu_4N_{16}O_{3.5}S_8W_2$	$C_{58}H_{72}B_2Cu_4N_{18}S_8W_2$
Fw	920.64	1744.16	1921.40
Crystal system	monoclinic	triclinic	triclinic
Space group	$P2_1/n$	$P\bar{1}$	$P\bar{1}$
a [Å]	17.980(4)	10.427(2)	10.602(2)
b [Å]	18.858(4)	11.489(2)	13.143(3)
c [Å]	20.417(4)	15.812(3)	13.876(3)
α [°]		72.43(3)	87.52(3)
β [°]	105.79(3)	83.51(3)	78.22(3)
γ [°]		77.19(3)	71.27(3)
V [Å^3]	6661(2)	1758.7(6)	1792.0(7)
Z	8	1	1
$D_{calcd.}$ [g cm^{-3}]	1.836	1.640	1.781
F(000)	3616	846	948
μ(Mo-K_α) [cm^{-1}]	4.995	4.727	4.646
Total number of reflections	32215	16934	5941
Number of unique reflections	11909 (R_{int} = 0.0820)	6383 (R_{int} = 0.0528)	5941 (R_{int} = 0.0610)
Number of variables	776	356	422
R[a]	0.0834	0.0572	0.0468
R_w[b]	0.1479	0.1523	0.0922
GOF[c]	1.138	1.070	0.907
Residual peaks and holes [e/Å^3]	1.046/–1.470	1.023/–1.011	0.449/–0.457

[a] $R_1 = \Sigma||F_o| - |F_c||/\Sigma|F_o|$. [b] $wR_2 = \{w\Sigma(|F_o| - |F_c|)^2/\Sigma w|F_o|^2\}\}^{1/2}$. [c] GOF = $\{\Sigma w(|F_o| - |F_c|)^2/(n-p)\}^{1/2}$, where n is the number of reflections and p is the total number of parameters refined.

18 H, CH_3 in Tp*), 2.48–2.50 (t, 4 H, -CH_2- in bpp), 3.02 (s, 18 H, CH_3 in Tp*), 6.53 (s, 6 H, CH in Tp*), 7.34–7.35 (d, 4 H, CH in bpp), 8.49–8.50 (d, 4 H, CH in bpp) ppm; the B-H proton signal was not located.

X-ray Structure Determinations: X-ray-quality single-crystals of **2**–**4** were obtained directly from the above preparations. All measurements were made with a Rigaku Mercury CCD X-ray diffractometer by using graphite-monochromated Mo-K_α (λ = 0.71070 Å). Each single crystal was mounted at the top of a glass fiber and cooled to 193 K in a stream of gaseous nitrogen. Cell parameters were refined by using the program CrystalClear (Rigaku and MSc, version 1.3, 2001) on all observed reflections. The collected data were reduced with CrystalClear. The reflection data were also corrected for Lorentz and polarization effects.

The structures of **2**, **3**·3.5H_2O, and **4** were solved by direct methods and refined on F^2 by full-matrix least-square techniques with the SHELXTL-97 program.[17] Because of the partial evaporation of the H_2O solvent molecules in **3**·3.5H_2O, the site-occupation factors for O1, O2–O4 atoms were fixed at 0.25 and 0.5, respectively. The crystal of **4** was found to be twinned by merohedry. The twin matrix was obtained by the Rotax or the TwinRotmat sub-program in Platon.[18a] The new HKL file with HKLF5 format was produced by the MAKE HKLF5 sub-program in WinGX.[18b] After application of the respective twin matrix for a pseudo merohedric twin, the *R*/*Rw* values dropped from 0.0770/0.2119 to 0.0468/0.0922. For **2**, **3**·3.5H_2O, and **4**, all non-hydrogen atoms, except those of the H_2O solvent molecules in **3**·3.5H_2O, were refined anisotropically. Hydrogen atoms on the oxygen atoms of the water solvent molecules in **3**·3.5H_2O were not located. Other hydrogen atoms were placed in geometrically idealized positions [C–H = 0.98 Å, with U_{iso}(H) = 1.5U_{eq}(C) for methyl groups; C–H = 0.99 Å, with U_{iso}(H) = 1.2U_{eq}(C) for methylene groups; C–H = 0.95 Å, with U_{iso}(H) = 1.2U_{eq}(C) for aromatic rings] and constrained to ride on their parent atoms. Important crystal and data collection parameters for **2**, **3**·3.5H_2O, and **4** are summarized in Table 2.

CCDC-666263 (for **2**), -666264 (for **3**·3·5H_2O), -666265 (for **4**) contain the supplementary crystallographic data for this paper. These data can be obtained free of charge from the Cambridge Crystallographic Data Center via http://www.ccdc.cam.ac.uk/data_request/cif.

Acknowledgments

This work was supported by the National Natural Science Foundation of China (20525101 and 20871088), the State Key Laboratory of Organometallic Chemistry of Shanghai Institute of Organic Chemistry (08-25), the Jiangsu Province for Higher Education (Qin-Lan Project and Program for Nature Science Key Basic Research), and the Suzhou University (Soochow Scholar Program and Program for Innovative Research Team).

[1] a) A. Müller, D. M. Dartmann, C. Rommer, W. Clegg, G. M. Sheldrick, *Angew. Chem. Int. Ed. Engl.* **1981**, *20*, 1060–1061; b) M. A. Ansari, J. A. Ibers, *Coord. Chem. Rev.* **1990**, *100*, 223–266; c) Y. Jeannin, F. Séheresse, S. Bernes, F. Robert, *Inorg. Chim. Acta* **1992**, *198–200*, 493–505; d) X. T. Wu, P. C. Chen, S. W. Du, N. Y. Zhu, J. X. Lu, *J. Cluster Sci.* **1994**, *5*, 265–285; e) H. W. Hou, X. Q. Xin, S. Shi, *Coord. Chem. Rev.* **1996**, *153*, 25–56; f) J. P. Lang, S. J. Ji, Q. F. Xu, Q. Shen, K. Tatsumi, *Coord. Chem. Rev.* **2003**, *241*, 47–60; g) Y. Y. Niu, H. G. Zheng, H. W. Hou, X. Q. Xin, *Coord. Chem. Rev.* **2004**, *248*, 169–183; h) X. T. Wu, *Inorganic Assembly Chemistry*, Science Press and Science Press USA Inc., Beijing, **2004**, pp. 1–179; i) C. Zhang, Y. L. Song, X. Wang, *Coord. Chem. Rev.* **2007**, *251*, 111–141.

[2] a) E. I. Stiefel, K. Matsumoto (Eds.), *Transition Metal Sulfur Chemistry, Biological and Industrial Significance*, *ACS Symposium Series 653*, American Chemical Society, Washington, DC, **1996**; b) G. N. George, I. J. Pickering, E. Y. Yu, R. C. Prince, S. A. Bursakov, O. Y. Gavel, I. Moura, J. J. G. Moura, *J. Am. Chem. Soc.* **2000**, *122*, 8321–8322; c) H. Dobbek, L. Gremer, R. Kiefersauer, R. Huber, O. Meyer, *Proc. Natl. Acad. Sci. USA* **2002**, *99*, 15971–15976; d) M. Ginda, R. Ferner, L. Gremer, O. Meyer, W. Meyer-Klaucke, *Biochemistry* **2003**, *42*, 222–230; e) G. N. George, I. J. Pickering, H. H. Harris, J. Gailer, D. Klein, J. Lichtmannegger, K. H. Summer, *J. Am. Chem. Soc.* **2003**, *125*, 1704–1705; f) M. Takuma, Y. Ohki, K. Tatsumi, *Inorg. Chem.* **2005**, *44*, 6034–6043.

[3] a) S. Shi, W. Ji, S. H. Tang, J. P. Lang, X. Q. Xin, *J. Am. Chem. Soc.* **1994**, *116*, 3615–3616; b) S. Shi, W. Ji, J. P. Lang, X. Q. Xin, *J. Phys. Chem.* **1994**, *98*, 3570–3572; c) H. G. Zheng, W. Ji, M. L. K. Low, G. Sakane, T. Shibahara, X. Q. Xin, *J. Chem. Soc., Dalton Trans.* **1997**, 2357–2362; d) S. Shi in *Optoelectronic Properties of Inorganic Compounds* (Eds.: D. M. Roundhill, J. P. Fackler Jr.,), Plenum Press, New York, **1998**, pp. 55–105; e) B. J. Coe in *Comprehensive Coordination Chemistry II* (Eds.: J. A. McCleverty, T. J. Meyer), Elsevier Pergamon, Oxford, U. K., **2004**, vol. 9, pp. 621–687.

[4] a) A. Müller, H. Bögge, U. Schimanski, *Inorg. Chim. Acta* **1983**, *69*, 5–16; b) F. Secheresse, F. Robert, S. Marzak, J. M. Manoli, C. Potvin, *Inorg. Chim. Acta* **1991**, *182*, 221–228; c) J. P. Lang, W. Y. Zhou, X. Q. Xin, J. H. Cai, B. S. Kang, K. B. Yu, *Polyhedron* **1993**, *12*, 1647–1653; d) H. W. Hou, D. L. Long, X. Q. Xin, X. Y. Huang, B. S. Kang, P. Ge, W. Ji, S. Shi, *Inorg. Chem.* **1996**, *35*, 5363–5367; e) J. P. Lang, H. Kawaguchi, K. Tatsumi, *Chem. Commun.* **1999**, 2315–2316; f) J. P. Lang, C. M. Jiao, S. B. Qiao, W. H. Zhang, B. F. Abrahams, *Inorg. Chem.* **2005**, *44*, 3664–3668; g) H. Yu, W. H. Zhang, Z. G. Ren, J. X. Chen, C. L. Wang, J. P. Lang, H. I. Elim, W. Ji, *J. Organomet. Chem.* **2005**, *690*, 4027–4035; h) J. P. Lang, Q. F. Xu, R. X. Yuan, B. F. Abrahams, *Angew. Chem. Int. Ed.* **2004**, *43*, 4741–4745; i) W. H. Zhang, Y. L. Song, Y. Zhang, J. P. Lang, *Cryst. Growth Des.* **2008**, *8*, 253–258; j) W. H. Zhang, J. P. Lang, Y. Zhang, B. F. Abrahams, *Cryst. Growth Des.* **2008**, *8*, 399–401; k) J. X. Chen, X. Y. Tang, Y. Chen, W. H. Zhang, L. L. Li, R. X. Yuan, Y. Zhang, J. P. Lang, *Cryst. Growth Des.* **2009**, *9*, 1461–1469; l) Y. J. Huang, Y. L. Song, Y. Chen, H. X. Li, Y. Zhang, J. P. Lang, *Dalton Trans.* **2009**, 1411–1421.

[5] a) J. P. Lang, Q. F. Xu, Z. N. Chen, B. F. Abrahams, *J. Am. Chem. Soc.* **2003**, *125*, 12682–12683; b) Q. F. Xu, J. X. Chen, W. H. Zhang, Z. G. Ren, H. X. Li, Y. Zhang, J. P. Lang, *Inorg. Chem.* **2006**, *45*, 4055–4064; c) J. P. Lang, Q. F. Xu, W. H. Zhang, H. X. Li, Z. G. Ren, J. X. Chen, Y. Zhang, *Inorg. Chem.* **2006**, *45*, 10487–10496; d) L. Song, J. R. Li, P. Li, Z. H. Li, T. Li, S. W. Du, X. T. Wu, *Inorg. Chem.* **2006**, *45*, 10155–10161; e) W. H. Zhang, Y. L. Song, Z. G. Ren, H. X. Li, L. L. Li, Y. Zhang, J. P. Lang, *Inorg. Chem.* **2007**, *46*, 6647–6660; f) K. Liang, H. G. Zheng, Y. L. Song, Y. Z. Li, X. Q. Xin, *Cryst. Growth Des.* **2007**, *7*, 373–376; g) W. H. Zhang, Y. L. Song, Z. H. Wei, L. L. Li, Y. J. Huang, Y. Zhang, J. P. Lang, *Inorg. Chem.* **2008**, *47*, 5332–5346.

[6] Y. Liu, Y. H. Mei, X. Q. Xin, W. T. Wong, *Transition Met. Chem.* **1999**, *24*, 81–84.

[7] H. Seino, Y. Arai, N. Iwata, S. Nagao, Y. Mizobe, M. Hidai, *Inorg. Chem.* **2001**, *40*, 1677–1682.

[8] J. Wang, Z. R. Sun, L. Deng, Z. H. Wei, W. H. Zhang, Y. Zhang, J. P. Lang, *Inorg. Chem.* **2007**, *46*, 11381–11389.

[9] a) Z. H. Wei, H. X. Li, M. L. Cheng, X. Y. Tang, Y. Chen, J. P. Lang, Y. Zhang, Z. R. Sun, *Inorg. Chem.* **2009**, *48*, 2808–2817; b) Z. H. Wei, H. X. Li, Z. G. Ren, J. P. Lang, Y. Zhang, Z. R. Sun, *Dalton Trans.* **2009**, 3425–3433.

[10] a) J. P. Lang, Q. F. Xu, W. Ji, H. I. Elim, K. Tatsumi, *Eur. J. Inorg. Chem.* **2004**, 86–92; b) F. J. Gao, H. Z. Zhu, X. Q. Xin,

A. B. Dai, W. X. Liu, B. Y. Wang, P. J. Zheng, *Chem. J. Chin. Univ.* **1990**, *11*, 1045–1048.
[11] a) M. Sherk-Bahae, A. A. Said, T. H. Wei, D. J. Hagan, E. W. Van Stryland, *IEEE J. Quantum Electron.* **1990**, *26*, 760–769; b) M. Sherk-Bahae, A. A. Said, E. W. Van Stryland, *Opt. Lett.* **1989**, *14*, 955–957.
[12] L. Yang, R. Dorsinville, Q. Z. Wang, P. X. Ye, R. R. Alfano, R. Zamboni, C. Taliani, *Opt. Lett.* **1992**, *17*, 323–325.
[13] a) Z. R. Chen, H. W. Hou, X. Q. Xin, K. B. Yu, S. Shi, *J. Phys. Chem.* **1995**, *99*, 8717–8721; b) C. Zhang, Y. L. Song, G. C. Jin, G. Y. Feng, Y. X. Wang, S. S. S. Rag, H. K. Fun, X. Q. Xin, *J. Chem. Soc., Dalton Trans.* **2000**, 1317–1323.
[14] a) H. G. Zheng, J. L. Zhou, M. F. Lapper, Y. L. Song, Y. Z. Li, X. Q. Xin, *Eur. J. Inorg. Chem.* **2004**, 2754–2755; b) Z. G. Ren, H. X. Li, G. F. Liu, W. H. Zhang, J. P. Lang, Y. Zhang, Y. L. Song, *Organometallics* **2006**, *25*, 4351–4357.
[15] a) J. Swiatkiewicz, P. N. Prasad, B. A. Reinhardt, *Opt. Commun.* **1998**, *157*, 135–138; b) O. K. Kim, K. S. Lee, H. Y. Woo, K. S. Kim, G. S. He, J. Swiatkiewicz, P. N. Prasad, *Chem. Mater.* **2000**, *12*, 284–286.
[16] a) W. H. Zhang, J. X. Chen, H. X. Li, B. Wu, X. Y. Tang, Z. G. Ren, J. P. Lang, Z. R. Sun, *J. Organomet. Chem.* **2005**, *690*, 394–402; b) S. Shi, W. Ji, W. Xie, S. H. Tang, H. C. Zeng, J. P. Lang, X. Q. Xin, *Mater. Chem. Phys.* **1995**, *39*, 298–303; c) C. Zhang, Y. L. Song, F. E. Kühn, Y. Xu, X. Q. Xin, H. K. Fun, W. A. Herrmann, *Eur. J. Inorg. Chem.* **2002**, 55–64; d) B. Wu, W. H. Zhang, H. X. Li, Z. G. Ren, J. P. Lang, Y. Zhang, Y. L. Song, *J. Mol. Struct.* **2007**, *829*, 128–134.
[17] a) G. M. Sheldrick, *SHELXS-97, Program for Solution of Crystal Structures*, University of Göttingen, Germany, **1997**; b) G. M. Sheldrick, *SHELXL-97, Program for Refinement of Crystal Structures*, University of Göttingen, Germany, **1997**.
[18] a) L. J. Farrugia, *J. Appl. Crystallogr.* **1999**, *32*, 837–838; b) A. L. Spek, *J. Appl. Crystallogr.* **2003**, *36*, 7–13.

Received: May 10, 2009
Published Online: August 20, 2009

